Coordination Chemistry Reviews, 47 (1982) 125–164
Elsevier Scientific Publishing Company, Amsterdam – Printed in The Netherlands

THERMOCHROMIC PHASE TRANSITIONS IN TRANSITION METAL SALTS

D.R. BLOOMQUIST and R.D. WILLETT

Department of Chemistry, Washington State University, Pullman, WA 99164 (U.S.A.)

(Received 15 January 1982)

CONTENTS

A. INTRODUCTION

A thermochromic material is one which changes color as the temperature is varied. In many cases, the thermochromism is a continuous effect showing a gradual color change over a wide temperature range due to changes in absorption band widths. A more interesting class of compounds involves a discontinuous color change associated with the onset of a first- or second-order structural phase transition. This review is restricted to inorganic transition metal salts which display discontinuous thermochromism. This change in spectra is associated with a change in coordination geometry or ligand field strength. It is known that metal ions can form salts with different coordination geometries in the solid state, depending upon the nature of the counter-ion influencing, for example, differences in hydrogen-bonding capabilities and crystalline packing forces. Thus, Mn^{2+} assumes an octahedral geometry in $(C_2H_5)_4NMnCl_3$ [1] but a tetrahedral geometry in $[(CH_3)_4N]_2MnCl_4$ [2]. In fact, both geometries can coexist in the same salt under appropriate circumstances, such as in $[(CH_3)_3NH]_3Mn_2Cl_7$ [3]. Through the study of compounds such as these, much can be learned about the forces that stabilize various coordination geometries. These results are always open to the suspicion, however, that the full nature of the forces which determine crystal structures is not really understood.

Thermochromic materials, then provide ideal systems to study changes in coordination geometry and/or ligand field strength since there is no change in counter-ion in the structure during the phase transition. All changes must be associated with changes in the strengths of interactions in the crystal brought about by the effect of temperature. This frequently means the onset of a (new) dynamic mode of motion in the structure. Thus, by studying the structures of the two crystalline phases and the dynamic behavior of the chemical entities above and below the structural phase transition, it should be possible to deduce clearly the crucial structural interactions which lead to the preference for a given geometry.

Unfortunately, as will be seen in this review, very few complete investigations of both static and dynamic properties have been made on thermochromic materials. It is clear that both types of information are needed, as conclusions drawn on the basis of only partial information are frequently erroneous. It is hoped that this review will inspire additional study of this colorful class of materials.

B. NICKEL DIMER–MONOMER TRANSITIONS

Several Ni(II) salts have been described recently which display structural isomerism of the form

$$[\mathrm{Ni(LL)Cl_2}]_2 \rightleftharpoons 2\ \mathrm{Ni(LL)Cl_2}$$

where LL is a bidentate nitrogen-bonding ligand [4–6]. These are listed in section (a) of Table 1. The dimer structure is yellow or orange and contains two Ni(II) ions, each with square-pyramidal coordination, while the monomeric species is characterized by pseudo-tetrahedral coordination geometry, distorted by the "bite" angle of the bidentate ligand.

In each case, the yellow dimeric compound undergoes a first-order cooperative transition into its violet isomer at a critical temperature. The transition is not strictly reversible, in that the reverse transition (if it occurs) takes place at a temperature well below the transition temperature. This type of behavior can be interpreted in terms of thermal hysteresis.

(i) Dichloro[trans-2-(2′-quinolyl)methylene-3-quinuclidinone]nickel(II)

The most thoroughly studied compound in this series is Ni(qnqn)Cl_2 and its dimeric isomer [Ni(qnqn)$Cl_2]_2$ where qnqn is *trans*-2-(2′-quinolyl)methylene-3-quinuclidinone [4,7–12].

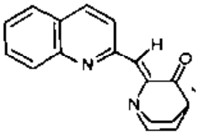

qnqn

This compound was first reported in 1970. The violet isomer is synthesized by adding a boiling solution of qnqn in butanol to a solution of $NiCl_2 \cdot 6H_2O$ in boiling 95% ethanol, followed immediately by rapid cooling in an ice bath [4]. The yellow isomer is prepared by dissolving the violet compound in methylene chloride, followed by slow evaporation to dryness at room temperature [8]. Both isomers are stable indefinitely at room temperature.

When a sample of the yellow isomer is heated in a sealed melting point tube, the color of the complex changes to violet over a 20° temperature range centered at 230°C [8]. The resulting violet complex has an X-ray powder pattern identical to that of the violet complex prepared directly. When cooled slowly from room temperature, the color returns to yellow over a temperature range of about 15° centered at −78°C. Both transitions can be interpreted as first order in that individual single crystals undergo the

TABLE 1

Thermochromism review summary

Compound	Transition temp. (°C)	Color change	Chromophore geometry change	Ref.
(a) Nickel dimer–monomer transitions				
Ni(qnqn)Cl_2	20, −78 [a]	Yellow–violet	square-pyramidal chloro-bridged dimer–distorted tetrahedral monomer	4, 7–12
Ni(dpm)Cl_2	220, 130	Orange–deep purple	square-pyramidal chloro-bridged dimer–distorted tetrahedral monomer	13
Ni(dmp)Cl_2	180	Yellow–purple	square-pyramidal chloro-bridged dimer–distorted tetrahedral monomer	5, 12, 14
(b) Compounds containing N,N-diethylethylenediamine				
$Cu(dieten)_2ClO_4$	45	Red–blue-purple	square-planar–disordered square-planar	17–26
$Cu(dieten)_2BF_4$	20	Red–purple	square-planar–disordered square-planar	17–19
$Cu(dieten)_2NO_3$	150	Red–violet	square-planar–disordered square-planar	19
$Ni(dieten)_2ClO_4$	110	Orange-yellow–bright red	square-planar–disordered square planar	17, 19
$Ni(dieten)_2BF_4$	95	Orange-yellow–bright red	square-planar–disordered square-planar	19
(c) Thermochromic copper(II) and nickel(II) halide complexes				
$(nmpH)_2CuCl_4$	80	Green–yellow	square-planar–distorted tetrahedral	30

$(IPA)_2CuCl_4$	55	Green–golden yellow	square-planar mono-bridged polymer–tetrahedral monomer	37–42
$(IPA)CuCl_3$	85	Brown–orange	square-planar bi-bridged dimer–octahedral tri-bridged polymer	41, 43
$(IPA)CuBr_3$	78		square-planar bi-bridged dimer–octahedral tri-bridged polymer	43
	100		octahedral tri-bridged polymer–tetrahedral mono-bridged polymer	
$(DEA)_2CuCl_4$	50	Bright green–bright yellow	square-planar–distorted tetrahedral	27, 43, 49, 51
$(pipzH \cdot HCl)_2CuCl_4$	80–95	Green-yellow–bright yellow	square-planar–distorted tetrahedral	29
$(pipzH \cdot HBr)_2CuBr_4$	80–95	Red-violet–bright red	square-planar–distorted tetrahedral	29
$(pipzH \cdot HCl)_2CuBr_4$	80–95	Red–bright red	square-planar–distorted tetrahedral	29
$(pipzH \cdot HCl)_2CuCl_3Br$	80–95	Red-orange–bright red-orange	square-planar–distorted tetrahedral	29
$(Me_3N_2H_2)_2NiCl_4$	145	Yellow–deep blue	tetragonally distorted octahedral–distorted tetrahedral	52
$(Me_3N_2H_2)_2NiBr_4$	70	Yellow–blue	octahedral–tetrahedral	
$(R_xNH_{4-x})_2NiCl_4$	70–200	Yellow–blue	tetragonally distorted octahedral–distorted tetrahedral	31
(d) Non-reversible thermochromism				
$(meth)_2NiBr_2$	20	Yellow–blue	octahedral–tetrahedral	59
$[CrCl_2(en)(pn)]Cl \cdot 0.75\ H_2O$	200	Green–violet	*trans*-octahedral–*cis*-octahedral	60
$[CrCl_2(pn)(tn)]Cl \cdot H_2O$	220	Green–violet	*trans*-octahedral–*cis*-octahedral	60
$[CrCl_2(en)(tn)](H_5O_2)Cl_2$	235	Green–violet	*trans*-octahedral–*cis*-octahedral	60
$[CrBr_2(pn)(tn)](H_5O_2)Br_2$	195	Green–violet	*trans*-octahedral–*cis*-octahedral	60
$Pd(iso\text{-}nma)_2$	100	Orange-red–blackish red	square-planar (N chelated)–square-planar (with one O chelated)	61
$Pd(iso\text{-}nea)_2$	100	Dark red–blackish red	square-planar (N chelated)–square-planar (with one O chelated)	61

TABLE 1 (continued)

Compound	Transition Temp. (°C)	Color change	Chromophore geometry change	Ref.
(e) Miscellaneous thermochromic compounds				
$Cu(NO_2)_2(NH_3)_2$	35	Green–purple	penta-coordinate (O chelated)–octahedral (N chelated)	62–64
$CuCl_x(NO_2)_{2-x}(NH_3)_2$	−40 to 30	Green–purple	penta-coordinate (O chelated)–octahedral (N chelated)	64
$Cu(nbv)_2 \cdot 2H_2O$	60	Lilac–blue	square-planar –distorted octahedral	65
$Cu(dmpd)_2(NO_3)_2$	~150	Red–violet	distorted octahedral–distorted square planar(?)	67
Cu_2HgI_4	66–71	Red–black	tetrahedral–disordered tetrahedral	68
Ag_2HgI_4	45–52	Yellow–red-orange	tetrahedral–disordered tetrahedral	68–72
Hg_2HgI_4	173	Yellow-orange–red	tetrahedral–disordered tetrahedral	68
$HgHgI_4$	126–127	Scarlet–yellow	tetrahedral–disordered tetrahedral	68
Tl_2HgI_4	116–187	Orange–scarlet	tetrahedral–disordered tetrahedral	68
$PbHgI_4$	134	Orange-red–yellow	tetrahedral–disordered tetrahedral	68

---

[a] Second number refers to the reverse transformation temperature.

structural transitions within a short time span (about 1 s) over a very narrow (about 0.1°C) range of temperature. The values of ΔH for the monomer to dimer transition [Ni(qnqn)Cl_2] (s, violet) → 1/2 dimeric{[Ni(qnqn)Cl_2]$_2$} (s, yellow) has been estimated at -2.60 kcal mol^{-1} from calorimetric measurements of heats of solution in 0.1 N HCl [11]. Thus, the yellow dimer structure is interpreted as being the thermodynamically more stable isomer below the thermochromic transition temperature, $T_{th} = 230$°C.

The crystal structure of the yellow dimer, determined by single-crystal X-ray diffraction techniques [9], is illustrated in Fig. 1. The dimer contains two nickel atoms with approximately square-pyramidal coordination with a crystallographic center of inversion requiring both pyramids to be identical with their apicies pointing in opposite directions. Two slightly asymmetric bridging halide ions share equatorial sites, while the bidentate ligand oc-

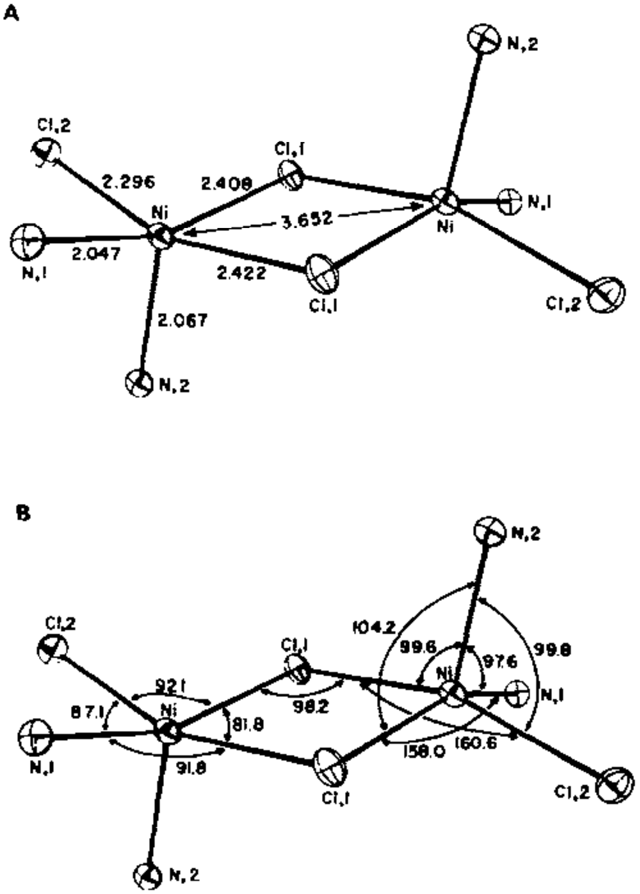

Fig. 1. The dimeric formula unit for [Ni(qnqn)Cl_2]$_2$.

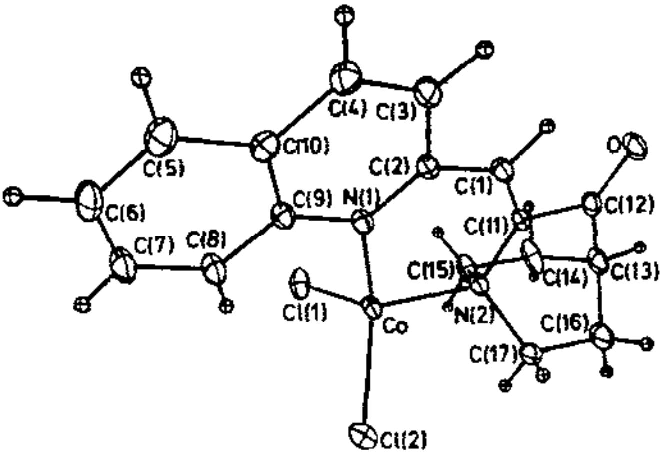

Fig. 2. The monomeric formula unit in Co(qnqn)Cl_2.

cupies the apical coordination position and one of the equatorial sites. The remaining equatorial site is occupied by a terminal chloride ion. The chelation ring shows significant distortion from planar geometry and highly anisotropic thermal parameters. The ligand bite angle is reported at 97.65(9)°.

Since single crystals of the violet isomer of sufficient size for X-ray work could not be obtained, the structure determination of the cobalt complex Co(qnqn)Cl_2 was undertaken [10]. This is shown in Fig. 2. The X-ray powder patterns of the two compounds are similar, however the two structures are not isomorphous. Co(qnqn)Cl_2 consists of cobalt(II) ions coordinated in a pseudo-tetrahedral manner to the two nitrogen-donor atoms in the ligand and to the two chloride ions. In the pseudo-tetrahedral cobalt complex, the bite angle is 100.35(9)°.

The data may be interpreted in the following manner. When the yellow dimeric complex, $[Ni(qnqn)Cl_2]_2$, is heated to about 230°C, sufficient vibrational energy is provided to break the two bridging chlorine bonds and to form the monomeric violet $[Ni(qnqn)Cl_2]$ complex. The monomer, if it resembles $[Co(qnqn)Cl_2]$, is characterized by a highly planar qnqn configuration which does not easily revert to the non-planar configuration required in the dimeric phase. The transition of the violet monomer to the yellow dimer requires movement and alignment of the molecules prior to the formation of the dimer, providing an activation barrier that is principally entropic rather than energetic. As a result, the transition (violet → yellow) is not particularly favored by high temperatures (between −70 and 230°C). The violet isomer is thus metastable at room temperature. At approximately −80°C, the decrease in unit cell size and thermal vibrations, and the accompanying changes in lattice packing, initiate the reformation of the bridging Ni–Cl bonds and the change in the conformation of the qnqn ligand.

Using a diamond anvil cell, Long and Ferraro [7] have shown that about 2 kbar pressure causes the violet isomer to change irreversibly to the yellow isomer at room temperature. The transformation is confirmed by visual inspection and low-frequency IR spectral evidence. This behavior is consistent with the argument presented above. It is interesting to note that Co(qnqn)Cl_2 also undergoes a reversible high-pressure structural change.

(ii) Dibromo[trans-2-(2′-quinolyl)methylene-3-quinuclidinone]nickel(II)

This compound, Ni(qnqn)Br_2, is prepared in the same manner as Ni(qnqn)Cl_2 [8]. It is violet and isostructural with the violet monomer Ni(qnqn)Cl_2. The corresponding yellow bromide dimer has not been observed, and no unusual thermal behavior has been reported.

(iii) Dichloro[trans-2-(6′-methoxy-2′-quinolyl)methylene-3-quinuclidinone]-nickel(II)

This is simply the 6′-methoxy derivative of the Ni(qnqn)Cl_2 compound described above. Both the violet and yellow isomers can be prepared at room temperatures as was possible for Ni(qnqn)Cl_2 [8]. Spectral data indicate that the structures are similar to those of Ni(qnqn)Cl_2, but no detailed study could be located. These isomers do not show any sign of thermal interconversion at either high or low temperatures.

(iv) Dichloro[bis(3,5-dimethylpyrazolyl)methane]nickel(II)

Stoichiometric amounts of $NiCl_2 \cdot 6H_2O$ and bis(3,5-dimethylpyrazolyl) methane [13] (abbreviated to dpm) in acetone will react yielding orange crystals of $[Ni(dpm)Cl_2]_2$ upon slow evaporation [6]. The properties of the compound are very similar to those of the qnqn salt. Above $T_{th} = 220°C$, a color change from orange to deep purple occurs accompanied by drastic changes in X-ray line patterns. A discontinuity in magnetic moment is observed at the transition with the moment increasing suddenly from 3.59 to 3.71 BM. The heat content of the orange → purple transition has been estimated at 2.5 kcal mol^{-1} of monomer using DTA measurements. Upon cooling to 130°C, the orange color and original X-ray powder diffraction pattern return demonstrating thermal hysteresis again, although less pronounced than in the qnqn salt.

Solid-state spectral data for the orange compound are in agreement with its formulation as a dimer with square-pyramidal geometry for the Ni(II). Low-temperature magnetic susceptibility measurements indicate considerable interaction between Ni(II) ions, in agreement with a chloro-bridged dimer model. Additional evidence for the chloro-bridged dimer structure comes from the far-IR spectra where the bridging Ni–Cl vibration is observed at 210 cm^{-1}.

The purple isomer almost certainly has a pseudo-tetrahedral geometry again. Spectral data on the salt dissolved in CH_2Cl_2 (purple solution) agree with a distorted tetrahedral geometry. Powder X-ray diffraction data show that the purple isomer is not isomorphous with the tetrahedral $Co(dpm)Cl_2$ and $Ni(dpm)Br_2$ compounds; but this does not rule out a tetrahedral species.

(v) Dichloro(2,9-dimethyl-1,10-phenanthroline)nickel(II)

When a solution of 2,9-dimethyl-1,10-phenanthroline (abbreviated to dmp) in ethanol is added to an excess of $NiCl_2 \cdot 6H_2O$ in ethanol, green crystals of the monohydrate $[Ni(dmp)Cl_2] \cdot H_2O$ precipitate, which form the purple $Ni(dmp)Cl_2$ monomer [14] when dehydrated by heating. The yellow dimer can be obtained by rapid evaporation of a chloroform solution of the hydrate.

When a sample of the yellow dimer is heated to $T_{th} = 180°C$, a discontinuous color change to purple is observed [5]. The X-ray powder pattern and reflectance spectra also change discontinuously at the phase transition temperature. Magnetic susceptibility measurements have been made on the $[Ni(dmp)Cl_2]_2$ dimer [12], showing antiferromagnetic exchange characteristic of a dimeric species. Unlike the violet $Ni(qnqn)Cl_2$ salt, $Ni(dmp)Cl_2$ does not revert to its yellow dimeric isomer upon cooling to liquid nitrogen temperature.

Indirect structural evidence again supports the formulation of a dimeric low-temperature species and a tetrahedral geometry for the purple, high-temperature isomer. X-ray powder diffraction data show that the purple monomeric species is isostructural with $Zn(dmp)Cl_2$, for which the crystal structure is known [5,15,16]. In the latter, the metal atom shows severely distorted tetrahedral geometry, with the narrowest angle being the bite angle of the bidentate ligand of 81.5(3)°.

In the absence of suitable single crystals of the yellow dimer $[Ni(dmp)Cl_2]_2$, the crystal structure of the solvated compound, $[Ni(dmp)Cl_2]_2 \cdot CHCl_3$, grown by slow recrystallization from chloroform, was undertaken [14]. Since the solvated and unsolvated compound have identical visible reflectance spectra, it is assumed that the structures are similar. The dimer structure in $[Ni(dmp)Cl_2]_2 \cdot 2CHCl_3$ is completely analogous to $[Ni(qnqn)Cl_2]_2$, except that the distortion from square-pyramidal geometry is more severe, with a ligand bite angle of 81.7(4)° owing to the more rigid nature of the dmp ligand. It is believed that the difference in rigidity between qnqn and dmp is responsible for the absence of the monomer–dimer transition at low temperature. Unlike the qnqn ligand, the dmp ligand prevents the rearrangement of the monomer structure necessary for the formation of the dimer.

(vi) Summary

In conclusion, the driving forces for these transitions seem to be entropic in nature. The dimer → monomer transition is facile at high temperatures since once one of the bridging bonds is ruptured, the four-coordinate monomeric entities formed can rearrange toward a tetrahedral geometry, weakening the remaining bridge, and allowing the second nickel ion to likewise rearrange. The extreme hysteresis observed in these systems is related to the difficulty in getting two monomeric species to simultaneously reorient in order to form the dimeric species.

C. THERMOCHROMIC COMPOUNDS CONTAINING *N,N*-DIETHYLETHYLENEDIAMINE

An extremely interesting class of compounds which exhibit thermochromism are transition metal salts of the form M(*N,N*-diethylethylenediamine)$_2$(X)$_2$ [17–20], where M is Cu(II) or Ni(II) and X is an anion. The distinguishing feature for the series is the existance of two types of thermochromism. For certain anions, a gradual spectral change occurs as the temperature is raised. This type of continuous thermochromism is observed for anions which do not easily become disordered. These will not be discussed here. With anions capable of disorder (specifically ClO_4^-, BF_4^-, and NO_3^-), this process occurs discontinuously. Compounds displaying discontinuous thermochromism also show an endothermic transition in DSC experiments [19]. Figs. 3(a) and 3(b) summarize the type of thermochromic behavior observed for the copper and nickel salts studied by Fabbrizzi et al. It will be seen that the thermochromism in these salts is not due to a change in coordination geometry, as discussed in the previous section. Rather, it is caused by a change in the ligand field strength due to thermal motion. This change can either occur continuously or discontinuously, depending on whether the motion obeys Boltzman statistics or occurs cooperatively in a structural phase transition.

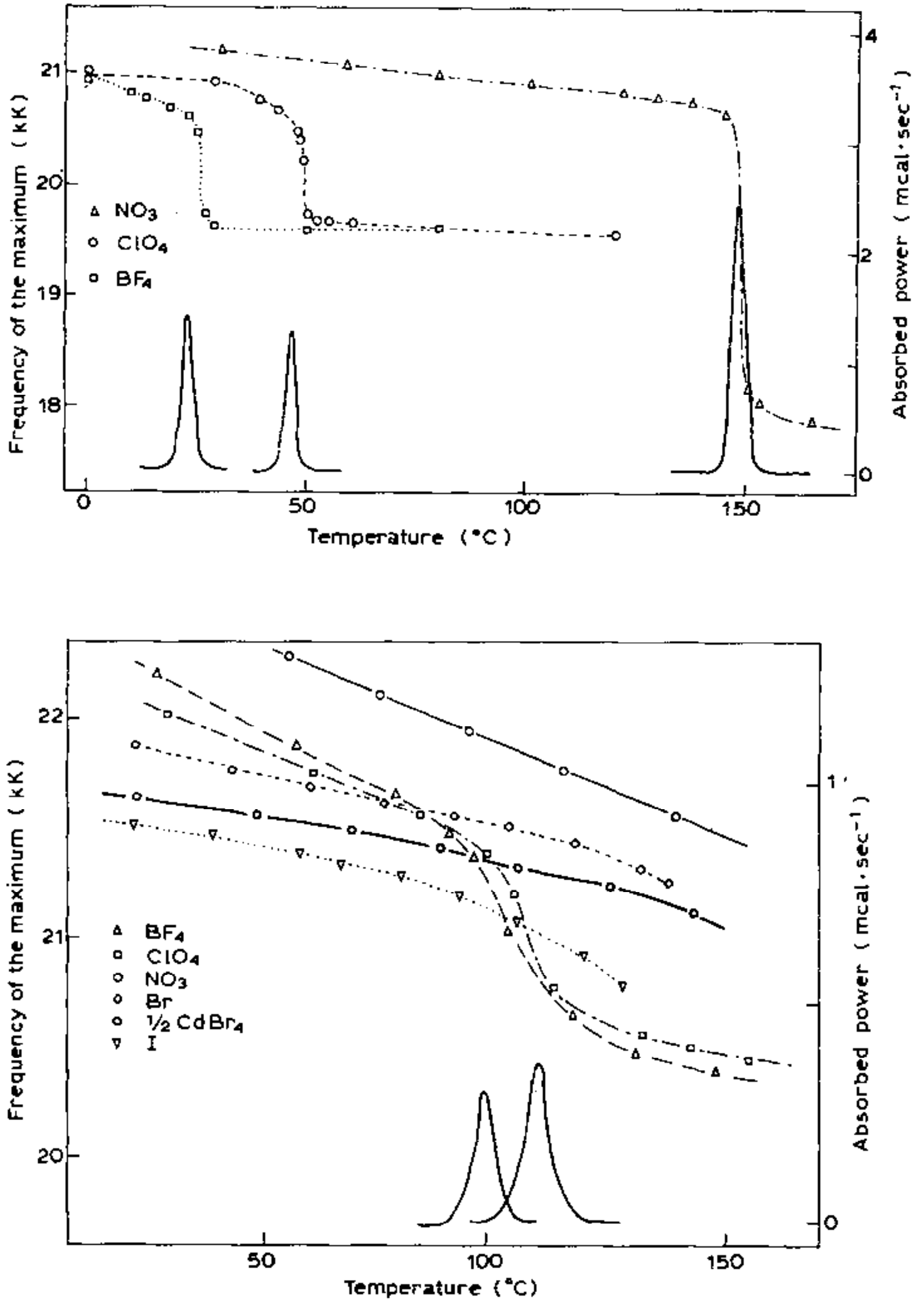

Fig. 3. DSC and visible electronic absorption maxima for (a) the Cu(dieten)$_2$X$_2$ salts and (b) the Ni(dieten)$_2$X$_2$ salts.

(i) *Bis(N,N-diethylethylenediamine)copper(II) perchlorate*

Bis(*N*,*N*-diethylethylenediamine)copper(II) perchlorate was first reported to be thermochromic in 1938 by Pfeiffer and Glaser [20]. The compound is red at room temperature and changes to deep blue-purple at $T_{th} = 43°C$, returning to red upon cooling. The value of ΔH for the first-order phase transition is 2.13 kcal mol^{-1} from integration of the DSC peak [19].

The crystal structures of both the red and the blue form have been reported [21,22]. The red room-temperature form crystallizes in the triclinic space group $P1$ with $Z = 1$, $a = 8.131(8)$, $b = 8.762(13)$, $c = 9.786(12)$ Å, $\alpha = 65.33(16)$, $\beta = 65.98(11)$ and $\gamma = 63.34(8)°$. The blue-violet form studied at 60°C is monoclinic, $I2$, with $Z = 4$, $a = 13.34(1)$, $b = 8.414(5)$, $c = 9.978(5)$ Å, and $\beta = 97.43(5)°$. The calculated densities of the low- and high-temperature forms are 1.51 and 1.48 respectively. No group–subgroup relationship exists between the two phases, and thus the transition must be first order.

The red room-temperature form of the copper(II) perchlorate salt (Fig. 4) has two molecules of *N*,*N*-diethylethylenediamine coordinated to the Cu(II) through the N atoms, which results in a square-planar CuN_4 geometry with

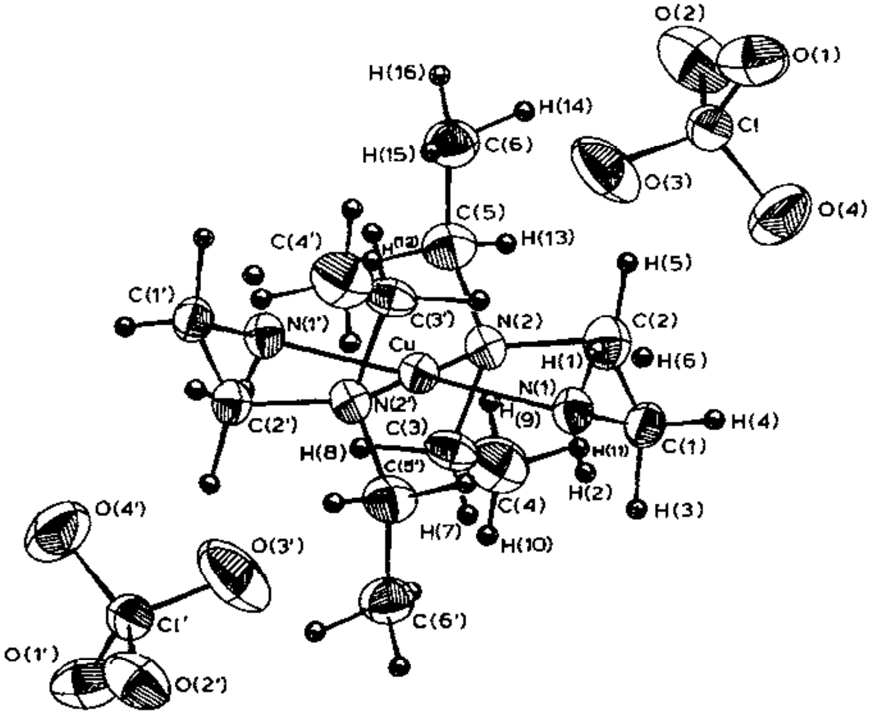

Fig. 4. The crystal structure of the red form (room-temperature) of $Cu(dieten)_2(ClO_4)_2$.

the Cu–NH_2 bonds being about 0.07 Å shorter than the Cu–NR_2 bonds. The two five-membered Cu–diamine rings adopt a symmetrical skew conformation and are related by a crystallographic inversion center located at the center of the complex. The ClO_4^- anions are isolated from the Cu(II) coordination sphere, with a closest Cu–O distance of 3.65(1) Å. However, each perchlorate ion is involved in two N–H · · · O hydrogen bonds with cations causing a slight distortion from perfect tetrahedral geometry.

In the high-temperature blue modification, the space group symmetry imposes a two-fold axis perpendicular to the $Cu(en)_2$ ring system, implying substantial changes in ring conformations accompanying the phase transition (Fig. 5). The structural analysis shows a $Cu(en)_2$ ring system which is nearly planar and contains some very short C–C bonds [1.37(2) Å] and large thermal amplitudes perpendicular to the ring. Both of these latter features are characteristic of the presence of disorder. The observed anisotropies of the thermal motion of the carbon atoms in the ethyl groups bonded to the ligand are also consistent with disorder. The perchlorate anion is again isolated with the shortest Cu–O bond length equal to 4.16(2) Å, 0.5 Å longer than in the room-temperature phase.

The solid-state NMR spectrum of the red isomer consists of two overlapping peaks, one being considerably broader than the other [22]. At the transition temperature, both lines show a 20–30% drop in linewidth, consistent with an averaging of the local magnetic fields by rapid ring inversion. Thus the disorder is certainly dynamic in nature.

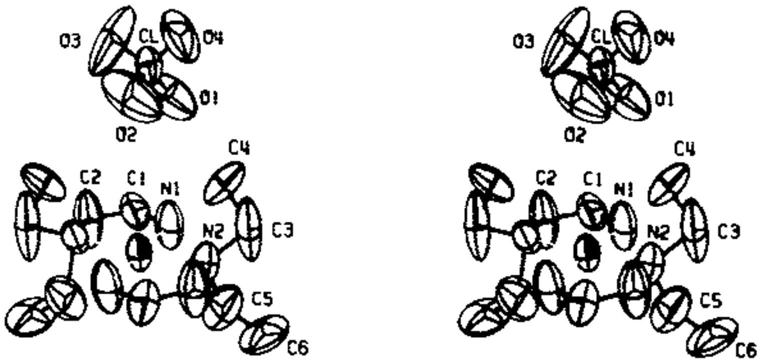

Fig. 5. The crystal structure of the blue form (high-temperature) of $Cu(dieten)_2(ClO_4)_2$.

Yokoi et al. [24], have examined the EPR of bis(*N*,*N*-diethylethylenediamine)copper(II) perchlorate extensively at various temperatures. A temperature dependence of the *g* values was observed, particularly for $g_{\parallel}$ which is 2.171, 2.156, and 2.117 at 80, 22, and −196°C in polycrystalline samples. This dependence was ascribed to an increase in the in-plane ligand field strength with decreasing temperature. The change in ligand field strength was thought to be due to decreasing axial interactions as the temperature is lowered. Lever et al. [18,25] examined temperature-dependent IR, far-IR and electronic spectra of the copper(II) perchlorate salt and interpreted these data according to a temperature-dependent axial interaction in agreement with Yokoi et al. Ferraro et al. [23] also interpreted this temperature and pressure dependent mid-IR data in terms of axial interactions and distortion of the metal atom environment. The thermochromic mechanism, postulated to involve the increase of an axial interaction between the perchlorate anion and the nickel complex, above the transition temperature, must be reformulated in the light of the crystal structure data presented above.

A study of the temperature dependence of the IR spectrum of bis(*N*,*N*-diethylethylenediamine)copper(II) perchlorate in the region 900–1250 cm^{-1} indicates that the perchlorate anion is not involved in partial covalent bonding in either form [17]. Spectra recorded at temperatures from 26 to 50°C are nearly identical, the main feature being a broad intense band at 1087 cm^{-1} assigned to the asymmetric stretching mode of the tetrahedral perchlorate anion. The crystal structures reported above are in complete agreement with these data showing isolated tetrahedral perchlorate anions in both phases.

It is concluded, then, that the thermochromic change in bis(*N*,*N*-diethylethylenediamine)copper(II) perchlorate must be due to a sudden change of the in-plane ligand field strength caused by conformational changes in the Cu(en)_2 ring system. In the low-temperature phase, the conformation allows optimal overlap of the nitrogen lone pair with the metal *d* orbitals. As the temperature is raised, a point is reached at which the thermal motion energy sufficiently weakens the hydrogen bonding network to allow the two Cu–diamine ring systems to begin rapid conformational interconversion. Although the Cu–N distances remain nearly constant, the disorder prevents optimal Cu–N overlap, causing a sudden decrease of the in-plane field strength. The resulting red shift in the visible absorption band of the copper complex is responsible for the change in color from red to purple at the transition temperature. This mechanism was first suggested by Hatfield et al., fourteen years before either crystal structure was completed [17].

(ii) Bis(N,N-diethylethylenediamine)copper(II) tetrafluoroborate

The tetrafluoroborate salt displays behavior very similar to that observed for the perchlorate salt [19]. The red to purple transition occurs at or below room temperature, which possibly prevented earlier experimenters from noticing the thermochromism [17]. Using a 1° min^{-1} scan rate, the DSC endotherm first deviates from the baseline at 15°C and is centered at about 20°C. The value of ΔH has been estimated to be 2.40 kcal mol^{-1}. A plot of the frequency of maximum absorption versus temperature for the BF_4^- salt shows a discontinuity identical to that found for bis(N,N-diethylethylenediamine)copper(II) perchlorate but occurs approximately 20° lower in temperature. In both salts, the maximum absorption frequency drops from 21000 cm^{-1} to about 19500 cm^{-1} at the transition temperature.

Although crystal structures of the isomers of the tetrafluoroborate salt are not available, it is likely that the complex is isomorphous with, or at least similar to, the perchlorate salt described in detail above. Some of the data collected for this compound have been interpreted according to Lever's tetragonal distortion model [18], but a more likely mechanism, considering the above discussion for bis(N,N-diethylethylenediamine)copper(II) perchlorate, involves a weakening of the in-plane ligand field strength with no axial interactions with the anion.

(iii) Bis(N,N-diethylethylenediamine)copper(II) nitrate

Of the compounds in this section, bis(N,N-diethylethylenediamine) copper(II) nitrate displays the highest thermochromic phase transition temperature ($T_{th} = 160°\text{C}$) and the highest ΔH_{trans} (4.18 kcal mol^{-1}) [19]. The thermochromic behavior, as well as the DSC experiment, is reversible; the exotherm obtained upon cooling exactly mirrors the endotherm seen while heating.

Most of the studies reported on this compound have been interpreted in terms of Lever's tetragonal distortion model [18]. Infrared spectra in the 1700–1800 cm^{-1} region are consistent with a transformation from a red four-coordinate square-planar complex to a purple six-coordinate isomer containing monodentately bound nitrate groups [18]. The red isomer shows a single sharp band at 1750 cm^{-1}, while the purple modification exhibits two weaker bands at 1748 and 1760 cm^{-1}.

In view of the abnormally large ΔH_{trans} and much more pronounced red shift in bis(N,N-diethylethylenediamine)copper(II) nitrate, (the maximum absorption frequency drops from 21000 cm^{-1} to below 18000 cm^{-1} at the thermochromic transition temperature), it is quite likely that this transition is different from those observed for the perchlorate and tetrafluoroborate described above. The IR results offer strong evidence that the anion plays a part in this transition and indeed, is probably coordinated in the high-temperature phase. A nitrate axial interaction is necessary to explain the more severe decrease in in-plane ligand field strength reflected in the large red shift.

In the room-temperature phase, the nitrate group may be involved in hydrogen bonding with the complex cations, perhaps similarly to the perchlorate salt. Possibly, as the complex is heated, thermal motion weakens the hydrogen-bonding network until a temperature is reached at which the nitrate slips into an axial coordination site, allowing the $Cu(en)_2$ ring system to become disordered. The superior hydrogen bonding ability of the NO_3^- group could explain the unusually high transition temperature in bis(*N*,*N*-diethylethylenediamine)copper(II) nitrate, and the severe anion rearrangement is compatible with the much larger ΔH and larger red shift than those observed for the tetrafluoroborate and the perchlorate salts.

Although further speculation as to a feasible mechanism should be postponed until crystal structure data are available, it is interesting to note that a similar compound, with somewhat less steric crowding, has been shown to contain octahedrally coordinated anions. The crystal structure of bis(*N*,*N*-dimethylethylenediamine)nickel(II) nitrite contains a roughly planar $Ni(en)_2$ ring system with oxygen bound NO_2^- groups in axial positions [10]. Considerable distortion from perfect octahedral geometry is observed.

(iv) Bis(N,N-diethylethylenediamine)nickel(II) perchlorate

Bis(*N*,*N*-diethylethylenediamine)nickel(II) perchlorate is orange-yellow at room temperature and changes discontinuously to bright red as the temperature is raised above transition temperature [19]. The DSC endotherm is somewhat broader than that observed for the copper(II) salts previously discussed. At a scan rate of 1° min^{-1} the DSC peak first deflects from the base line at 110°C; the integrated area gives an estimated ΔH_{trans} of 1.59 kcal mol^{-1}. Although complete crystal structures are not available, similarities in the *d* spacings and relative intensities in the powder patterns of bis(*N*,*N*-diethylethylenediamine)copper(II) and -nickel(II) perchlorates indicate that the two compounds are isomorphous [17]. The red shift in bis(*N*,*N*-diethylethylenediamine)nickel(II) perchlorate is not as dramatic as that observed for the copper(II) complexes. The maximum absorption frequency changes from about 21500 to 20500 cm^{-1} over a 20° range. The thermochromic mechanism is assumed to be the same as that of the copper(II) perchlorate discussed in detail in that section.

(v) Bis(N,N-diethylethylenediamine)nickel(II) tetrafluoroborate

The behavior of the nickel(II) tetrafluoroborate is almost identical to that of the nickel(II) perchlorate, changing from orange-yellow to bright red at about 100°C [19]. The value of ΔH_{trans} has been estimated at 1.37 kcal mol^{-1}, and DSC experiments show that the transition first begins at 94°C. A plot of absorption maximum versus temperature is identical for both the perchlorate and the tetrafluoroborate salts. The proposed thermochromic mechanism is discussed in the copper(II) perchlorate section.

(vi) Bis(N,N-diethylethylenediamine)nickel(II) nitrate

Bis(*N*,*N*-diethylethylenediamine)nickel(II) nitrate does not display a thermochromic phase transition. The transition temperatures of the nickel complexes are about 70° higher than for the corresponding copper complexes. The predicted transition temperature for bis(*N*,*N*-diethylethylenediamine) nickel(II) nitrate is therefore about 220°C, which is higher than the decomposition temperature.

(vii) Summary

The thermochromism in this series of salts has been shown to be due to the weakening of the in-plane ligand field strength as the temperature is raised, not to an increase in the axial interactions (except possibly in the nitrate salt). This weakening of the ligand field strength is associated with a dynamic disorder of the *N*,*N*-diethylethylenediamine ligands. This mechanism would appear to be operative in both the continuous and discontinuous thermochromic salts. In the continuously thermochromic salts, this disorder is thermally activated, that is, it obeys Boltzman statistics. In the cases of discontinuous thermochromism discussed in this section, the disorder sets in suddenly at a well defined temperature.

The role of the anion in determining the behavior needs to be investigated further. It is reasonable to postulate that if the anion is capable of undergoing rotational disorder that the thermochromism is discontinuous. Conversely, if the anion is incapable of such disorder (a halide ion, or the very heavy CdBr_4^{2-} anion), then the only observed effect is the continuous thermochromic behavior.

D. THERMOCHROMIC COPPER(II) AND NICKEL(II) HALIDE COMPLEXES

A number of copper(II) chloride salts of the form $(\text{RNH}_3)_2\text{CuCl}_4$ display gradual thermochromism in the solid state [28]. The continuous thermochromic effect is attributed to a variation in the linewidths of the electronic absorption bands with temperature and will not be discussed here. Some more highly substituted amine cations form copper(II) chloride salts which undergo first-order phase transitions associated with the thermochromism [28–30]. A series of nickel(II) chlorides with a general formula $(R_xNH_{4-x})_2NiCl_4$ have also demonstrated discontinuous thermochromism [31]. In each case, the color change is associated with drastic changes in the metal–halide coordination geometry.

These metal–halide salts represent a distinctly different type of system from those discussed in Sections A and B. In those, the bidentate nature of the coordinating ligands imposed certain constraints on the type of processes which could occur. In particular, the bidentate "bite" angle was not disturbed during structural phase transitions. On the other hand, the simple metal–halide salts to be discussed in this section have no steric constraints imposed upon them, other than those inherent with the metal ion itself. Since the potential surface of the $CuCl_4^{2-}$ anion has been shown to have a very shallow minimum and the position of the minimum to be very sensitive to small changes in ligand field strength [27], it is anticipated that the copper halide salts should be susceptible to changes in coordination geometry. Thus, a wider (more colorful) array of behavior is anticipated, although, as will be seen, a common thread runs through the whole series of salts which have been examined.

(i) Bis(N-methylphenethylammonium) tetrachlorocuprate(II)

Bis(*N*-methylphenethylammonium) tetrachlorocuprate(II), hereafter abbreviated $(nmpH)_2CuCl_4$, changes discontinuously from green to yellow at 80°C [30]. Complete crystal structure results are available for both modifications of $(nmpH)_2CuCl_4$, revealing a dramatic change in $CuCl_4^{2-}$ geometry from square planar to flattened tetrahedral associated with the thermochromic transition, as shown in Fig. 6. The densities below and above the transition are 1.397 and 1.367 g cm^{-3} respectively. This is the simplest thermochromic copper halide system which has been studied to date.

At 25°C dark green needles of $(nmpH)_2CuCl_4$ belong to the space group $P2_1/c$ with $a = 6.4952(3)$, $b = 22.678(1)$, $c = 8.5844(6)$ Å, $\beta = 116.08(1)°$ and $Z = 2$. The $CuCl_4^{2-}$ anion is constrained to be planar by crystallographic symmetry requirements and contains angles of 90° within experimental error. The anions deviate from perfect square planar geometry only in that the Cu–Cl bond distances differ by 0.033 Å. Considerable hydrogen bonding is present between the $CuCl_4^{2-}$ anions and the amine cation. In the green modification, the cation is ordered but shows extreme thermal motion in the ring system.

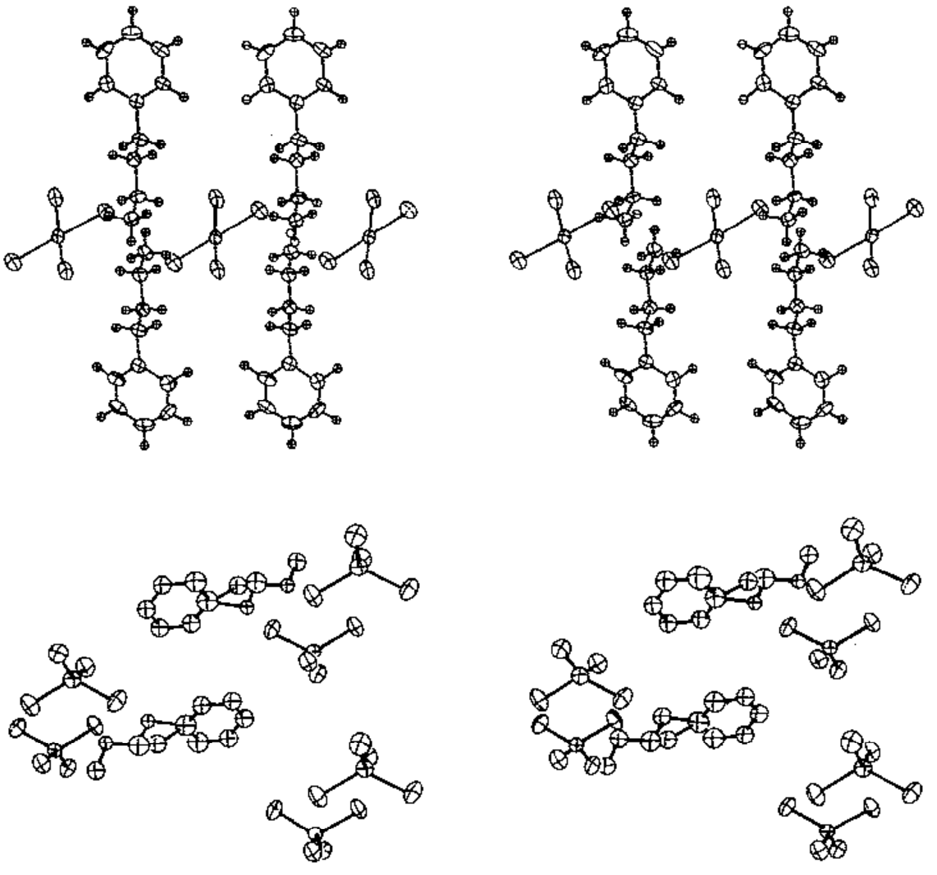

Fig. 6. The low-temperature (green) form (top) and the high-temperature (yellow) form (bottom) of $(\text{nmpH})_2\text{CuCl}_4$.

The yellow isomer belongs to the C-centered monoclinic cell $C2/c$ with $a = 24.93(3)$, $b = 8.180(7)$, $c = 12.586(8)$ Å, $\beta = 115.21(7)°$ and $Z = 4$. Data were collected at 80°C on a crystal grown from the melt. CuCl_4^{2-} ions in this phase lie on a two-fold rotation axis and display distorted tetrahedral geometry, the largest Cl–Cu–Cl angle being 138.1°. A weakening of the hydrogen-bonding network is observed, along with a corresponding shortening of Cu–Cl bonds. The nmpH cation shows extreme disorder except for the N atom which is held in place by hydrogen bonding.

The solid-state electronic spectrum taken below the transition temperature shows three distinct peaks at 16900, 14300 and 12500 cm^{-1}. The highest energy d–d transition in tetrachlorocuprate(II) anions with tetragonally distorted octahedral geometry are near 13000 cm^{-1}, and the square-planar complex $Pt(NH_3)_4CuCl_4$ has an absorption maximum at 14300 cm^{-1} [32–34]. An increase in the overall splitting of the *d*-orbitals is expected in an octahedral environment as the ligands on the *z* axis are gradually withdrawn, the limiting case being reached in the four-coordinate square-planar arrangement. The unusually high *d–d* transitions in the room-temperature phase of $(nmpH)_2CuCl_4$ are attributed to the isolated nearly perfect square-planar $CuCl_4^{2-}$ ions with no axial interactions. Above the thermochromic transition, the absorption spectrum consists of a single broad maximum at approximately 9100 cm^{-1}, which is consistent with tetrahedral symmetry. In solution, the complex also displays tetrahedral geometry.

The structural characteristics of this phase transition are quite simple, particularly in view of the copper halides to be discussed subsequently. Thus, it is worthwhile to examine its behavior in some detail and to seek to draw some conclusions concerning the cause of the transition. As has been noted [28,35], the stereochemistry of four-coordinate copper(II) halide salts is subject to a delicate balance between two effects; crystal field stabilization [favoring square-planar (D_{4h}) geometry] and ligand–ligand electrostatic repulsions [favoring a flattened tetrahedral (D_{2d}) geometry]. The electrostatic charge on the halides can be neutralized by interaction with neighboring cations. If the cation selected is a neighboring copper ion, a polymeric structure results. The interactions can also occur with the counter-ion present in the crystal. If this counter-ion is capable of undergoing dynamic disorder (as, for example, some organic cations), the possibility of changing the strength of the electrostatic interaction exists, leading to a change in coordination geometry.

Thus, in $(nmpH)_2CuCl_4$, the strong hydrogen bonding present in the low-temperature phase withdraws electron density from the chloride ion, and the crystal field stabilization dominates, leading to a simple square-planar geometry. At the phase transition, an onset of a (presumably) dynamic disorder of the substituted ammonium ion occurs. This weakens the hydrogen bonding, increasing the charge density on the chloride ions, and forcing the $CuCl_4^{2-}$ anions to distort towards a tetrahedral geometry. It will be seen that this basic argument will hold for all of the copper halide salts studied.

(ii) Bis(isopropylammonium) tetrachlorocuprate(II)

The thermochromic behavior of this salt was first mentioned by Remy and Laves in 1933 [36]. A virgin sample of the salt undergoes a green → yellow thermochromic transition at 55°C. For subsequent runs, T_{th} occurs at 50°C. This salt probably represents the next level of complexity for the thermochromic copper halide salts, in that the low-temperature phase has a polymeric structure, but the high-temperature phase contains discrete $CuCl_4^{2-}$ anions.

The triclinic structure of the green, needle-like crystals of phase II, reported by Anderson and Willett in 1974, is quite complex [37]. It contains two similar, but inequivalent, ribbons of $CuCl_4^{2-}$ ions running parallel to the crystallographic *c* axis. The structure of one of these ribbons is shown in Fig. 7. Each ribbon can be visualized as a section cut from the copper–chloride layer structure present in the typical laminar structures of $(RNH_3)_2CuCl_4$ salts [38]. (Indeed, upon application of high pressure, the salt converts to the laminar structure [39]). Each ribbon is sheathed with a layer of IPA ions, with strong N–H $\cdots$ Cl hydrogen bonding holding the cations to the ribbon and stabilizing the ribbon structure. The central $CuCl_4^{2-}$ anions in each ribbon retain the 4 + 2 coordination present in the laminar salts, completing their coordination spheres by forming bridges with the $CuCl_4^{2-}$ anions on the edges of the ribbons. Because of the disruption of the laminar structure, these anions have only a 4 + 1 coordination, and exhibit a small, but definite, tetrahedral distortion.

The high-temperature (yellow phase) structure has recently been determined by Bloomquist and Willett [40]. The salt is orthorhombic, *Pnma*, and contains discrete isolated distorted tetrahedral $CuCl_4^{2-}$ anions. The IPA cations are disordered, restricted by crystallographic mirror planes. The

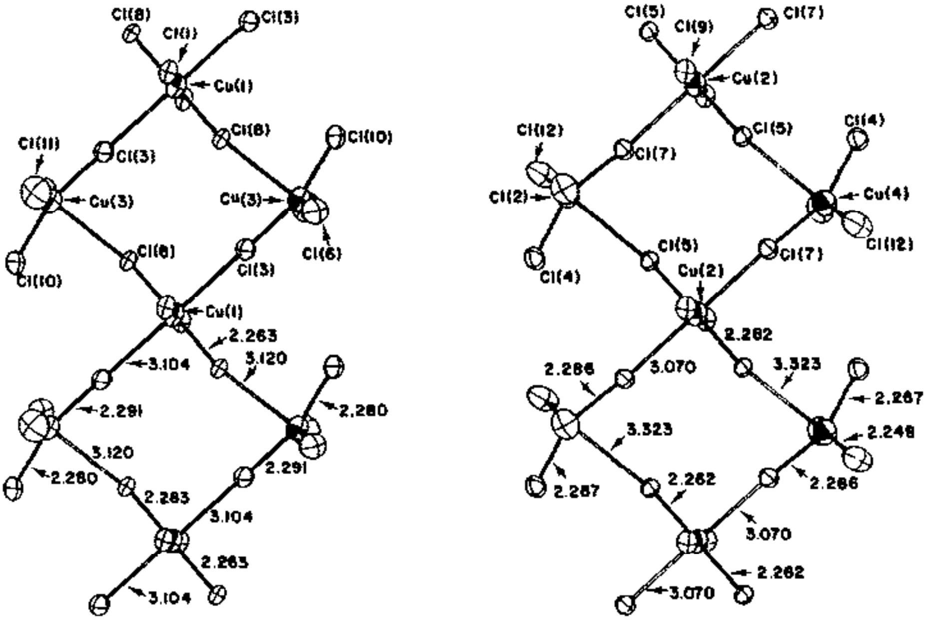

Fig. 7. An illustration of the two $CuCl_4^{2-}$ ribbons in $(IPA)_2CuCl_4$.

N–H ··· Cl distances increase, indicating a weakening of the hydrogen-bond structure. This weakening reduces the amount of charge withdrawal from the chloride ions, increasing electrostatic ligand–ligand repulsion and favoring the distorted tetrahedral conformation over the planar geometry in the green phase.

The *d–d* absorption bands occur at lower energy in the high-temperature phase. The broad, featureless *d–d* band shifts discontinuously from 11000–13000 cm^{-1} in phase II to 10000 cm^{-1} in phase I. This leads to the initial postulate of a tetrahedral geometry for the high-temperature phase [28], which has been confirmed by the X-ray diffraction study.

The far-IR region of the spectrum has also been investigated for both phases, as well as for the pressure stable phase [39]. The b_2 vibration (D_{2d} symmetry) is particularly sensitive to the extent of tetrahedral deformation of the CuCl_4^{2-} anion. This band occurs at 232 cm^{-1} in phase I and shifts to 181 cm^{-1} in phase II. The *e* vibration, which occurs at 290 cm^{-1} in phase I, splits into two bands at 271 and 301 cm^{-1} in phase II. This splitting is presumably due to the presence of both planar and slightly distorted CuCl_4^{2-} anions in phase II. This region collapses to a 281 cm^{-1} band with a weak shoulder in the pressure stabilized phase.

Magnetic susceptibility studies show a small (2%) [41] increase in the magnetic moment at T_{th}. This is primarily due to the larger moment associated with the tetrahedral coordination geometry in phase I. The susceptibility of quenched phase I shows the existence of very weak antiferromagnetic interactions [40], while the dominant interactions for phase II are ferromagnetic [42]. The EPR *g* tensor and linewidths also change discontinuously at T_{th} [40].

The temperature dependence of the NMR linewidth confirms the existence of a dynamic disorder of the IPA cations in the high-temperature

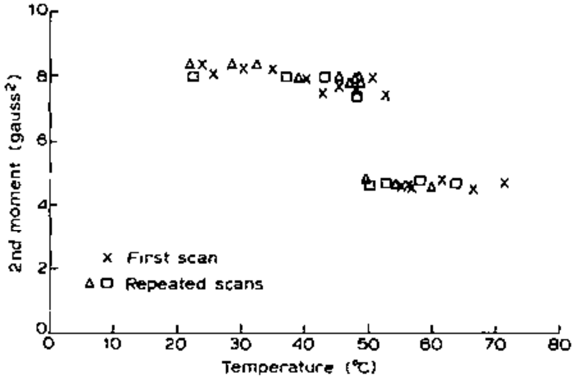

Fig. 8. Temperature dependence of the second moments of the ^{1}H NMR line in $(\text{IPA})_2\text{CuCl}_4$.

phase. The second moment of the resonance line drops discontinuously from 7.8 Oe^2 to 4.8 Oe^2 at the phase transition (Fig. 8), in good quantitative agreement with predictions based on the disorder observed in the crystal structure. Again, this occurs at 55°C on initial runs, but at 50°C upon repeated heating. This is consistent with the complexity of the structural change, in that the low-temperature phase never regains its total crystalline integrity upon cooling back through the transition.

The driving force of the phase transition is postulated to be entropic in nature. The onset of the dynamic disorder of the organic cation weakens the hydrogen bonding, thus forcing the $CuCl_4^{2-}$ anions to undergo a tetrahedral distortion. The stereochemistry of the room-temperature phase is stabilized by a combination of strong hydrogen bonding and electrostatic interactions with neighboring copper ions. The polymeric structure is broken up during the phase transition, yielding a structure containing isolated $CuCl_4^{2-}$ anions.

(iii) Isopropylammonium trichlorocuprate(II)

This salt has been studied in extensive detail in our laboratory [43]. It undergoes a first-order phase transition at $T_{th} = 51°C$, with the color changing from a brown to orange. Single-crystal X-ray structure determination, ^1H NMR measurements, EPR and magnetic susceptibility studies have been carried out. These studies show that hydrogen bonding stabilizes a dimeric form of the complex in the room-temperature phase. At the phase transition, the isopropylammonium ion (IPA) becomes dynamically disordered, and the copper halide framework collapses into a tribridged linear chain system.

The salt, first reported by Remy and Laves [36] in 1933, is easily synthesized by reacting stoichiometric amounts of the amine hydrochloride and cupric chloride dihydrate in water, methanol or ethanol. Remy and Laves mentioned that the salt changed color upon heating, but unlike the diethylethylenediamine salts, it has attracted little attention or further work.

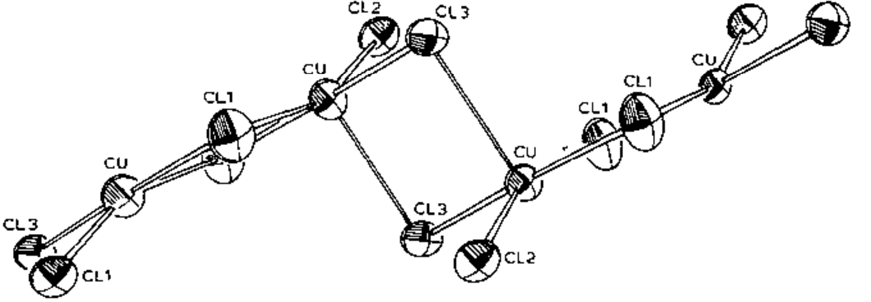

Fig. 9. The chain of dimers in the room-temperature form of $(IPA)CuCl_3$.

The structure of the room-temperature phase (phase II) will be described first. It is triclinic, $P\bar{1}$, with two formula units per unit cell. As seen in Fig. 9, the salt contains bibridged linear chains of $Cu_2Cl_6^{2-}$ dimers. The repeat distance along the chain is 6.106 Å. The dimer has the usual symmetric bibridged structure, with a distortion from planarity very similar to that found in $(CH_3)_2NH_2CuCl_3$ [44]. The compound exhibits the typical pleochroic behavior associated with dimeric copper salts, with the maximum absorption parallel to the Cu–Cu direction. Two of the terminal chloride ions in each dimer are involved in the formation of the asymmetrical bridges to the adjacent dimers. The IPA ions hydrogen bond strongly to the other two terminal chloride ions.

A single crystal of the phase II salt was slowly heated while mounted on the X-ray diffractometer. At approximately 50–55°C, the crystal converted to the high-temperature phase (phase I), remaining single during this transformation. Phase I is orthorhombic, *Pcan*, with four formula units per unit cell. The volume per formula unit decreases upon entering the high-temperature phase. The salt now contains tribridged linear chains of $(CuCl_3)_n^{n-}$ stoichiometry (Fig. 10), very similar to those found in $[(CH_3)_3NH]_3Cu_2Cl_7$ [45] and $(CH_3)_4NCuCl_3$ [46]. The chain orientation is coincident with the chain direction in phase II, the repeat distance having increased from 6.106 to 6.365 Å. Crystallographically, the IPA ions in phase I are required to sit

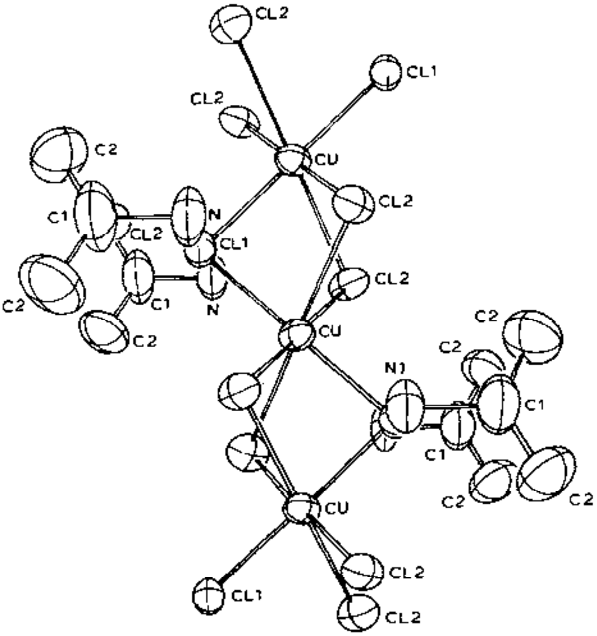

Fig. 10. The tribridged linear chain in the high-temperature form of (IPA)$CuCl_3$.

on a two-fold axis of symmetry, and thus must be disordered. The N–H ⋯ Cl hydrogen-bond distances increase significantly at the phase transition. The decrease in volume is associated with the transformation of the copper chloride linear chain from a bibridged system to a more compact tribridged system.

The structures of the two phases are very closely related to each other, despite the drastic change in coordination geometry that occurs during the transition. Comparison of a projection of the two structures onto the plane perpendicular to the chain axis reveals very little movement of the chains relative to each other, and the IPA ions occupy the same general locations.

The magnetic moment increases discontinuously by ~6% at T_{th} [40], as seen in Fig. 11. This increase is consistent with the geometrical changes which occur. The dimer exhibits antiferromagnetic coupling, while the tribridged linear chain system leads to strong ferromagnetic interactions [47].

DSC measurements give $\Delta H_{\text{th}} = 1.4$ kcal mol^{-1} and $\Delta H_{\text{melt}} = 6.5$ kcal mol^{-1}. Significantly, T_{th} increases by ~10°C for the partially deuterated salt, $(CH_3)_2CHND_3CuCl_3$, although ΔH_{th} and ΔH_{melt} remain unchanged. The increase in T_{th} upon deuteration is consistent with a weaker hydrogen bonding in phase I. Upon deuteration, the free energy of each phase will decrease by an amount equal to the difference in zero point vibrational energies. Since the hydrogen bonds are stronger in phase II, its free energy will decrease by a greater amount, thus stabilizing it with respect to phase I.

Measurements of the ^{1}H NMR spectrum were made as a function of temperature for both (IPA)$CuCl_3$ and the partially deuterated salt. The

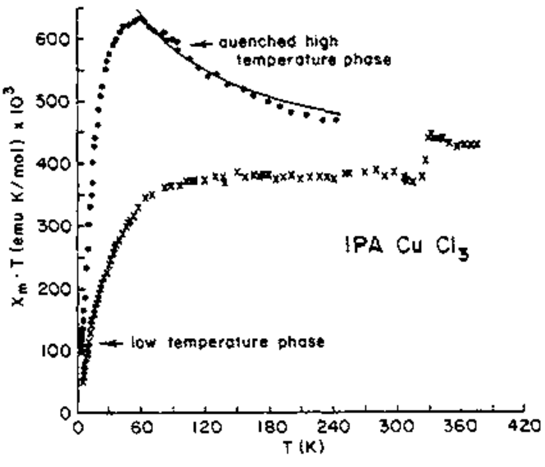

Fig. 11. A plot of $\chi_m T$ vs. T for the two phases of (IPA)$CuCl_3$.

linewidths of the partially deuterated salts were significantly narrower because of the absence of the spectrum of the NH_3 protons, which show a substantial contact shift. The linewidths for both salts drop by 30–40% at T_{th}. Again, the transition occurs 10° higher for the partially deuterated salt. The linewidths in phase I are compatible with an IPA ion undergoing a dynamic two-fold disorder.

A quite complete description of the mechanism can now be put together. The structure of phase II is stabilized by the strong hydrogen bonding of the IPA ion to the non-bridging chloride ions in the $Cu_2Cl_6^{2-}$ dimers. As the temperature is raised, the entropic contributions to the free energy of phase I increase to the point where they overcome the greater lattice stability of phase II. In the presence of weaker hydrogen bonding, the copper chloride framework stabilizes itself by involving all chloride ions in bridge formation. The strong role of cation–chloride ion hydrogen bonding is clearly demonstrated.

(iv) Isopropylammonium tribromocuprate(II)

The bromide analog of $(IPA)CuCl_3$ also undergoes structural phase transitions. As with all copper bromide salts, the existence of a strong charge-transfer absorption band in the middle of the visible region makes them essentially opaque, so the actual color change is difficult to determine.

The room-temperature structure of $(IPA)CuBr_3$ (phase III) has been determined [43b,48], and it is isomorphous with the room-temperature phase of the chloride salt. However, instead of undergoing one transition, experimental evidence indicates that two transitions exist. DSC results show two anomalies at 78 and 100°C, with the melt occuring at 143°C. The actual transition temperatures may be somewhat lower than these values due to the characteristic superheating observed for this type of salt. Thermodynamic values obtained are $\Delta H_{th1} = 1.3$ kcal mol^{-1}, $\Delta S_{th1} = 3.7$ e.u., $\Delta H_{th2} = 0.8$ kcal mol^{-1}, $\Delta S_{th2} = 2.2$ e.u., $\Delta H_{mp} = 5.0$ kcal mol^{-1}, and $\Delta S_{mp} = 12.0$ e.u. The thermodynamic values for the first transition agree very favorably with those for $(IPA)CuCl_3$.

Powder X-ray diffraction patterns corroborate the existence of a pair of structural phase transitions. The intermediate phase (phase II) of $(IPA)CuBr_3$ appears to be isomorphous with phase I of $(IPA)CuCl_3$ but a drastic change occurs in the power pattern upon conversion to phase I. It is proposed that the high-temperature phase contains a chain of singly bridged tetrahedral $CuBr_4^{2-}$ ions.

Magnetic susceptibility studies on quenched phase I indicate Curie–Weiss type behavior with weak antiferromagnetic coupling; the onset of three-dimensional magnetic ordering occurs at 6 K. This behavior is consistent with the proposed chain structure.

The existence of the second phase transition in (IPA)$CuBr_3$ provides an additional insight into the behavior of (IPA)$CuCl_3$ (and the first transition of (IPA)$CuBr_3$). In that transition, the halide ions offset the weakening of the hydrogen bonding by increasing the interaction with neighboring copper ions. However, the tribridged structure is sterically crowded, and as the disorder of the IPA ions increases, the copper halide structure relaxes to a distorted tetrahedral configuration that minimizes electrostatic repulsion between halide ions.

(v) Bis(diethylammonium) tetrachlorocuprate(II)

This salt, $(DEA)_2CuCl_4$, undergoes a thermochromic phase transition at 50°C, changing from bright green to bright yellow. Spectroscopic studies [28] have indicated this transition is associated with a change in coordination geometry of the $CuCl_4^{2-}$ anion from nearly square planar to distorted tetrahedral with a predicted *trans* Cl–Cu–Cl angle of 135°. Since there was no evidence of bridge formation in this salt, it was anticipated that the phase transition should be particularly simple. Structural investigations have shown this not to be the case.

Considerable thermal hysteresis, both on heating and cooling, exists. It is possible to keep supercooled samples of the high-temperature phase (phase I) at room temperature for several weeks. In fact, with very pure samples, it is possible to supercool the melt (m.p. = 93°C) down below the phase transition temperature and to crystallize phase II directly from the melt.

The structure of phase II has been determined by Simonsen [49]. The structure is monoclinic, $P2_1/n$, with $a = 7.632$, $b = 15.025$, $c = 45.193$ Å and $\beta = 89.94°$. It contains three crystallographically independent $CuCl_4^{2-}$ anions, as shown in Fig. 12, each with a different degree of tetrahedral distortion superimposed on the basic square-planar geometry. The average *trans* Cl–Cu–Cl angles are 178.5, 159.3 and 145.3°. The cations hydrogen bond to the anions, tying them together into a two-dimensional array. This is reflected in the magnetic properties, where the salt exhibits two-dimensional antiferromagnetism, with the hydrogen bonding providing the dominant superexchange pathway [50]. The reason for the difference in coordination geometry between the three anions is not clear, but presumably it has to do with small differences in hydrogen bonding to the three types of anions. The X-ray diffraction patterns show strong evidence of a sub-cell structure, corresponding to a division of the c axis repeat distance by a factor of three.

The high-temperature structure is also monoclinic, $P2_1/c$, with $a = 25.066$, $b = 10.565$, $c = 13.472$ Å and $\beta = 100.65°$. There are now two independent

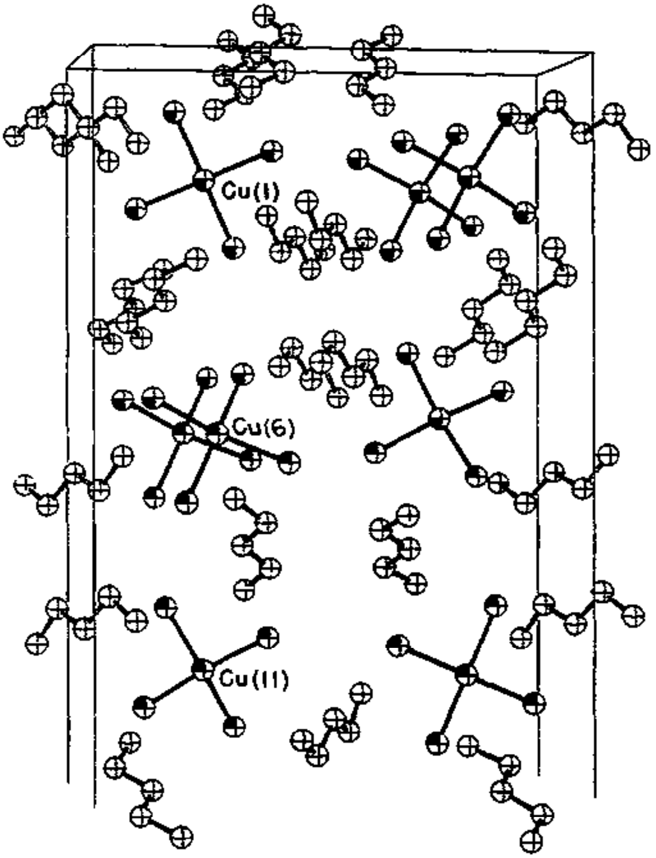

Fig. 12. The room-temperature structure of $(DEA)_2CuCl_4$.

$CuCl_4^{2-}$ anions per unit cell. No simple relationship between the structures of the two phases exists. The detailed structure of the high-temperature phase has not been elucidated, apparently due to disorder of one of the two independent anions. The anions show the expected distorted tetrahedral geometry.

DSC studies give $\Delta H = 3.5$ kcal mol^{-1} and $\Delta S = 10.8$ e.u. These values are significantly higher than the corresponding values for the phase transition in $[(C_2H_5)_2NH_2]_2ZnCl_4 \cdot x\ H_2O$ [24] which involved a two-fold disorder of the cations. It is argued that these data support the proposed disorder of the $CuCl_4^{2-}$ anion deduced from the X-ray study.

The second moment of the ^1H NMR resonance, shown in Fig. 13, shows a sharp (50%) drop at the phase transition. This drop proves that the transition involves an onset of a dynamic disorder of the DEA cation. It was not possible to deduce the type of disorder from these studies.

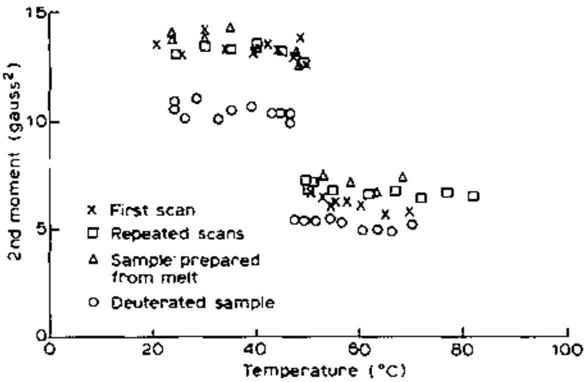

Fig. 13. The temperature dependence of the second moment of the ^{1}H NMR line for $(DEA)_2CuCl_4$.

The EPR spectrum of the low-temperature phase is typical of a magnetically coupled system [50], in accord with the conclusions of the magnetic studies. The EPR spectrum changes discontinuously at the phase transition to a spectrum which shows no evidence for magnetic coupling. Since the magnetic exchange is proposed to proceed via a hydrogen bridging superexchange mechanism, these results would indicate that the hydrogen bonding is substantially weakened in phase I.

(vi) Tetrahalo- and mixed tetrahalo-cuprates of the piperazinium dication

In a study of tetrahalo- and mixed tetrahalo-cuprates of the piperazinium dication, the following four compounds were synthesized which display discontinuous thermochromic behavior [28]: $(pipzH \cdot HCl)_2CuCl_4$, $(pipzH \cdot HPBr)_2CuBr_4$, $(pipzH \cdot HCl)_2CuBr_4$, and $(pipzH \cdot HCl)_2CuCl_3Br$. These complexes can be prepared by adding ether to an ethanolic solution containing stoichiometric amounts of the corresponding ions. At room temperature the compounds vary in color from green to red-violet as the Br content increases. Although no crystallographic data are available, room-temperature electronic spectra for each of these compounds reveal an intense *d–d* band near 11500 cm^{-1}, suggesting an approximately square-planar configuration [32]. Above the transition temperature of 80–95°C, the color intensifies and the *d–d* transitions shift to higher energies indicating a change to a distorted tetrahedral symmetry. The color change and spectral behavior are reversible. Far-IR data are also consistent with the indicated geometry changes.

The proposed mechanism for the thermochromism involves a weakening of the hydrogen bonding network as the temperature is raised. At room temperature, $N{-}H \cdots Cl$ hydrogen bonding draws electron density away from the chloride ions, allowing the effect of crystal field stabilization to prevail, hence the square-planar geometry. Above the transition temperature, thermal energy has weakened the hydrogen bonding and ligand–ligand repulsions dominate, forcing the less sterically crowded tetrahedral geometry.

(vii) Bis(trimethylhydrazinium) tetrachloronickelate(II)

The yellow complex bis(trimethylhydrazinium) tetrachloronickelate(II) can be obtained in crystalline form from ethanol [52]. When the complex is heated to 145°C, it undergoes a reversible first-order thermochromic transition to a deep blue isomer with identical composition. The reverse transformation occurs slowly at temperatures below 120°C. If the compound is heated above 220°C for a prolonged period, it disproportionates to form the pinkish tan $NiCl_3$ salt and the chloride salt of the ligand. Upon cooling, the yellow complex is eventually reformed proving that it is the most stable form at room temperature. The yellow isomer is assigned a tetragonally distorted octahedral coordination geometry on the basis of the electronic spectrum. The blue modification contains the familiar tetrahedral tetrachloronickelate(II) anion.

The analogous Br compound is yellow at room temperature and transforms sharply to the blue tetrahedral structure at 70°C. This isomerization is not reversible however, in that, upon cooling, the disproportionation product is obtained.

(viii) $(R_xNH_{4-x})_2NiCl_4$ *complexes*

A series of thermochromic complexes of Ni(II) of the type $(R_xNH_{4-x})_2NiCl_4$ have been reported where R is an alkyl or aryl group and x is 1 or 2 [31]. The compounds are prepared from the melt of 2:1 mole ratios of the amine hydrochloride and anhydrous $NiCl_2$. The complexes are brown-yellow to green-yellow at room temperature and change to royal blue or blue-green upon heating to the thermochromic temperature, which ranges from about 70°C to over 200°C depending on the cation chosen. Substituted ammonium cations with strong hydrogen-bonding ability (e.g. $CH_3NH_3^+$) tend to raise the thermochromic transition temperature and those with less hydrogen-bonding potential (e.g. Me_3NH^+) tend to yield lower transition temperatures.

Although single crystals suitable for crystallographic structure solution could not be obtained, X-ray diffraction patterns and far-IR spectra are characteristic of polymeric octahedral complexes. Magnetic susceptibility measurements at room temperature are also typical of octahedral nickel(II) complexes, the observed magnetic moments ranging over 2.9–3.4 BM [53–55]. Although the structure of the room-temperature polymeric material is not known, it is postulated that the polymer contains distorted $NiCl_6$ octahedra sharing bridging chlorine atoms.

Above the transition temperature, the blue compound shows a single far-IR absorption at 288 cm^{-1} which corresponds to a metal–chlorine stretching vibration in a tetrahedral $NiCl_4^{2-}$ ion [56,57]. The magnetic moments increase to about 3.8 BM at the transition temperature, consistent with a tetrahedral geometry around the Ni atoms. The proposed mechanism for the thermochromism involves a change in geometry and coordination numbers from an octahedral six-coordinate to a four-coordinate tetrahedral geometry.

It has been shown in our laboratory [58] that the process for the phase transition in $(C_3H_7NH_3)_2NiCl_4$ is substantially different from that proposed by Sherren and Ferraro [57]. X-ray powder diffraction studies indicate a process involving the disproportionation products at room temperature reacting at the thermochromic temperature to form the tetrahedral blue $NiCl_4^{2-}$ salt as follows

$$(C_3H_7NH_3)NiCl_3 + (C_3H_7NH_3)Cl \rightarrow (C_3H_7NH_3)_2NiCl_4$$

Upon cooling, the disproportionation products return. This behavior is analogous to that observed for bis(trimethylhydrazinium)tetrabromonickelate(II) described earlier. The trichloride powder diffraction pattern is consistent with a linear chain of face-shared octahedra as is found in $(CH_3NH_3)NiCl_3$. It is suspected that this process occurs for most of the nickel chloride salts of monoammonium cations.

These $(R_xNH_{4-x})_2NiCl_4$ complexes resemble the analogous copper(II) salts in some respects. When x is 0 or 1, the preferred geometry around the Cu atom is square planar, shifting to a distorted tetrahedral geometry for $x > 1$. In the nickel complexes, the favored geometry is distorted octahedral for $x = 1$ or 2, with tetrahedral symmetry stabilized for $x > 2$. In thermochromic systems containing either $NiCl_4^{2-}$ or $CuCl_4^{2-}$ anions, the strength of the hydrogen-bonding network governs the transition temperature.

E. NON-REVERSIBLE THERMOCHROMISM

Compounds discussed in this section undergo first-order phase transitions accompanied by changes in color as the temperature is raised. Unlike compounds discussed in previous sections, the reverse transformation is not observed as the temperature is lowered.

(i) Dibromobis(4-methylthiazole)nickel(II)

Dibromobis(4-methylthiazole)nickel(II) crystallizes as a blue complex from a methanol solution whereas the yellow isomer is obtained from ethanol [59]. The blue complex is isomorphous with the analogous cobalt compound and has been assigned tetrahedral coordination geometry on the basis of its electronic spectrum. It is assumed that the yellow form corresponds to an octahedral halogen-bridged complex with axial 4-methylthiazole groups. The magnetic moment of 2.98 BM is consistent with such a structure. The yellow isomer is classified as thermochromic, in that it reverts slowly to the blue form at room temperature and more rapidly at higher temperatures. The reverse transformation is not reported.

(ii) Mixed bis(diamine)chromium(III) complexes

Several mixed bis(diamine)chromium(III) complexes display non-reversible thermochromic behavior [60] including: *trans*-$[CrCl_2(en)(pn)]Cl \cdot 0.75 H_2O$, *trans*-$[CrCl_2(pn)(tn)]Cl \cdot H_2O$, *trans*-$[CrCl_2(en)(tn)](H_5O_2)Cl_2$ and *trans*-$[CrBr_2(pn)(tn)](H_5O_2)Br_2$. The *trans* isomer of each of these compounds is green and can be grown in crystalline form from concentrated hydrochloric or hydrobromic acid. The above compounds show endothermic DTA peaks at 200, 220, 235 and 195°C respectively, corresponding to a change in color from green to violet.

The thermochromic phase transition is associated with a one-way *trans*-to-*cis* isomerization. Activation energies for the transitions have been estimated to be 39, 45, 28 and 31 kcal mol^{-1} $degree^{-1}$, respectively. The proposed bond rupture mechanism involves an intermediate with three bromide ions arranged in *mer* positions and a singly bound bidentate ligand. Loss of one of the *trans* bromide ions followed by chelation of the bidentate ligand completes the isomerization.

(iii) Bis(isonitroso-β-ketoesterimino)palladium(II) complexes

Bis(isonitrosomethylacetoacetateimino)palladium(II) and bis(isonitrosoethylacetoacetateimino)palladium(II) grow as orange-red and dark red crystals from an aqueous methanol solution [61]. Upon heating to 100°C under reduced pressure, the compounds turn blackish red. When returned to room temperature, the blackish red color persists and elemental analysis indicated identical stoichiometry with the unheated compounds.

Both phases are diamagnetic, indicating square-planar palladium geometry. IR and ^1H NMR data provide convincing evidence that the low-temperature phase is characterized by a *trans* symmetric structure with the ligands coordinated through isonitroso nitrogens and imine nitrogens forming five-membered chelate rings. The mass spectra indicate that both isomers are monomeric.

When the compounds are heated above the thermochromic transition temperature, the IR spectra change drastically. The ester carbonyl and NH bands each split, suggesting a change in bonding of one of the coordinated ligands from isonitroso nitrogen to isonitroso oxygen, giving a hybrid six-membered chelate ring. This rare type of irreversible transformation is termed "thermochromic intramolecular chelate linkage isomerization."

F. MISCELLANEOUS THERMOCHROMIC COMPOUNDS

Compounds in this section display first-order thermochromism but cannot be readily classified under previous sections.

(i) Dinitrodiaminecopper(II)

This compound is one of the more intriguing thermochromic salts which has been reported, due to the fact that the transition temperatures can be tuned by changing the composition. Dinitrodiaminecopper(II) was first prepared by Bassett and Durrant [62] by thermal decomposition of dinitrotetraaminecopper(II). The thermochromic compound is green at 65°C and purple below 35°C [63]. Mori et al. [64] have found that T_{th} can be lowered by replacing some of the nitrite ions with Cl or Br. A continuous range of transition temperatures from about −40 to 30°C can be achieved by gradually increasing the percentage of Cl or Br doped into the complex. For Cl concentrations greater than 6% (weight percent Cl) or Br concentrations greater than 10%, the green form is stable at all temperatures above the liquid nitrogen temperature. The series of compounds described above were obtained in crystalline form from a water–methanol–ethyl acetate solvent.

Magnetic susceptibility and DTA measurements indicate that the transition is discontinuous. From X-ray powder diffraction data, it is evident that the green and purple isomers have different crystal structures. A shift of each diffraction maximum to higher angle is observed as the halide ion concentration is increased, indicating a decrease in the size of the crystal lattice.

Single-crystal diffraction studies of the green compound with the formula $CuCl_{0.17}(NO_2)_{1.83}(NH_3)_2$ indicate a monoclinic system with $a = 8.966$, $b = 7.529$, $c = 4.440$ Å and $\beta = 104.4°$. Preliminary refinement in the space group *Cm* with two formula units per unit cell suggests *trans* coordination of two ammonia ligands and O chelation of one nitrite ion.

An IR absorption peak at 425 cm^{-1}, appearing only in the spectrum of the purple form, was assigned as the $Cu{-}NO_2$ stretching mode on the basis of the expected shift to 415 cm^{-1} upon isotopic substitution with $^{15}NO_2$. N chelation in the purple form is confirmed by the presence of the symmetric NO_2 stretching mode not observed for the green compounds. Further evidence for N chelation in the green form is found in the electronic spectra. The green form (with O-coordinated NO_2) has an absorption peak at lower energy than the N-coordinated violet form, in conformity with the order in the spectrochemical series.

Although the complete crystal structures of the two forms are not known, it is postulated that the green form contains a penta-coordinate Cu ion with O chelated NO_2 groups. The purple form may have elongated octahedral stereochemistry with N coordinated NO_2 groups and the more distant coordination positions occupied by O atoms from adjacent complexes. The change in coordination is responsible for the thermochromism.

(ii) (N-benzyl-L-valinato)(N-benzyl-D-valinato)copper(II) dihydrate

The dihydrate of the *N*-benzyl-DL-valine copper(II) complex crystallizes from an aqueous methanol solution as lilac plates belonging to the monoclinic space group $P2_1/c$ with $a = 13.026(8)$, $b = 8.612(4)$, $c = 11.270(8)$ Å, $\beta = 99.60(3)°$ with two molecules per unit cell [65]. When the complex is heated to 60°C, a transition occurs to a triclinic blue isomer belonging to the space group $P\bar{1}$ with $a = 9.837(5)$, $b = 11.435(5)$, $c = 5.975(3)$ Å, $\alpha = 102.80(5)$, $\beta = 93.15(5)$, $\gamma = 95.20(5)°$, with one molecule per unit cell. Single crystals of the blue isomer suitable for X-ray studies were grown from absolute methanol at elevated temperatures. The structures are illustrated in Fig. 14.

In both phases, the copper ion is located on a crystallographic center of inversion bound to two *N*-benzyl-valinate anions. The anion acts as a bidentate ligand bonding through the N and O atoms. In the room-temperature phase, the chelate rings are severely distorted from planarity. The copper coordination geometry is square planar in the room-temperature phase, with steric crowding from the ligand system screening the copper atom axial coordination sites. The water molecules are hydrogen bonded to the ligands of adjacent complexes forming infinite chains parallel to the crystallographic *b* axis. In the blue, high-temperature modification, the chelate ring adopts a more nearly planar configuration with less axial crowding, allowing the water molecule to form a long axial bond with the Cu atom. The coordination octahedron of the copper atom in the blue phase is appreciably distorted, with the $Cu-OH_2$ bond forming an angle of 77° with the O–Cu–N plane. The thermochromism is a result of the rather drastic change in coordination geometry around the Cu chromophore.

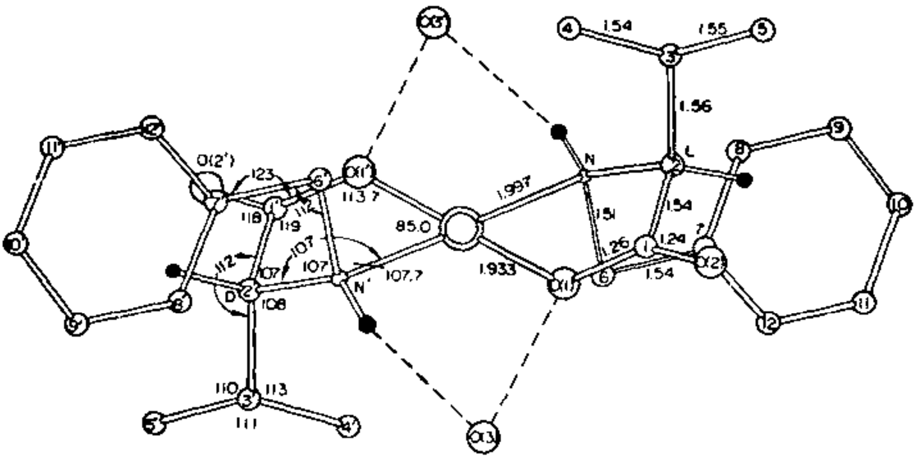

I

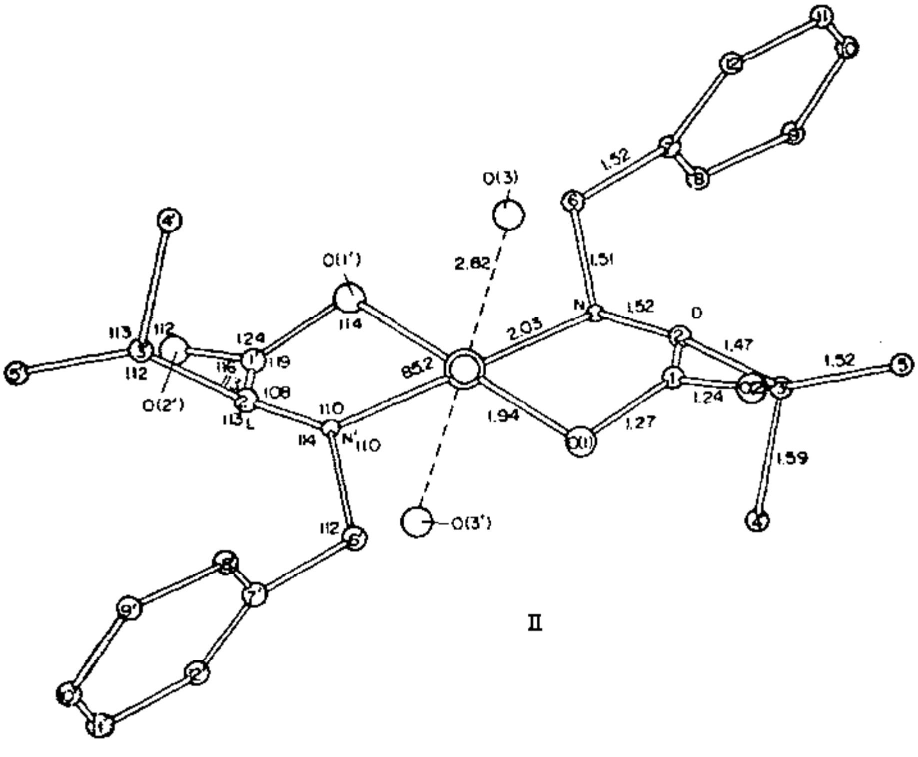

II

Fig. 14. The structures of the low-temperature (I) and high-temperature (II) forms of (*N*-benzyl-DL-valine)copper(II) dihydrate.

(iii) Propylenediamine complexes of Cu^{2+}

The thermochromic behavior of the series of salts $Cu(dmpd)_xX_2$, where dmpd ≡ 2,2-dimethylpropane-1,3-diamine and $X = Cl^-$, Br^-, ClO_4^- and NO_3^- have recently been reported. With $X = Cl^-$, Br^- or ClO_4^-, continuous thermochromism is observed, with a shift in the *d–d* absorption bands to lower energy as the temperature is raised [66]. For $X = NO_3^-$, a discontinuous type of behavior was observed [67].

The room-temperature crystal structure of $Cu(dmpd)_2(ClO_4)_2$ was determined as part of the study. The crystals were monoclinic, space group $P2_1/c$ with $a = 9.724(2)$, $b = 6.827(1)$, $c = 16.191(3)$ Å and $\beta = 97.66(1)°$. The centrosymmetric complex has a typical 4 + 2 square-bipyramidal geometry, with the four amine nitrogen atoms defining the basal plane and an oxygen from each of two coordinated perchlorates occupying the apical sites. The Cu–N distances average 2.024 Å and the Cu–O distances are 2.602 Å. Thus, in contrast to the $Cu(dieten)_2X_2$ salts, coordination of the anion does occur.

Spectroscopic investigations were carried out to determine the type of change in coordination geometry associated with the thermochromism. IR studies showed the splitting of the perchlorate bands decreased continuously with increasing temperature. This implies a change in symmetry of the ClO_4^- anion from C_{3v} at low temperature towards T_d at high temperatures. This, it is argued, when combined with the lowered *d–d* energies, implies a tetrahedrally distorted four-coordinate geometry at high temperatures. If so, the distortion must be dynamic in nature, involving torsional twisting of the pn rings, since the crystallographic symmetry requires the presence of a center of inversion.

The study of the discontinuous thermochromism in the NO_3^- salt ($T_{th} \sim 150°C$) will be particularly interesting, to see if the transition really does involve a process in which dissociation of the nitrate ions does occur during the phase transition.

(iv) Thermochromic tetraiodomercurates

A number of heavy-metal tetraiodomercurates have been shown to exhibit first-order thermochromic phase transitions [68]. The structure of the room-temperature phase of Ag_2HgI_4 has been determined by X-ray powder diffraction to be body-centered tetragonal with $a_0 = 6.32$ and $c_0 = 12.64$ Å [69,70]. Above the thermochromic transition temperature, the powder pattern is characteristic of a cubic lattice which corresponds to 1/2 of the room-temperature tetragonal unit cell [71]. The thermochromic transition has been shown to be an order–disorder transition with the cations ordered below the transition temperature and disordered above the phase transition temperature [72]. It is assumed that the other compounds undergo similar transitions.

Although some of these compounds have been known for over 100 years [73], the possible use of these compounds as erasable, high density IR recording devices has sparked renewed interest in recent years [74,75]. Of particular interest is the compound Cu_2HgI_4 which shows a reproducible hysteresis loop spanning about 20°. The reproducibility around the steep portions of the hysteresis loop makes this compound especially well suited for IR recording applications.

G. CONCLUSION

The phenomenon of inorganic thermochromism represents an interesting overlap of the area of solid-state physics and inorganic chemistry. What sets thermochromic materials apart from the many other systems which undergo phase transition is the readily identifiable change in an external physical property. As with many materials which undergo solid-state phase transitions, there certainly exists potential for practical application, although these have not been explored except for the mercuric iodide salts. Their use for such devices as temperature indicators, temperature sensitive light filters, etc. would seem worth exploring.

The study of these materials has been very useful in helping to understand the competitive nature of various factors which influence coordination stereochemistry in inorganic systems. The phenomenon clearly demonstrates the existence of different coordination geometries of very comparable energies. In classical inorganic stereochemistry, similar behavior is drawn from the existence of stereoisomers. Different isomers, however, often have quite different ground-state energies, the more unstable isomers being obtained only under preparative conditions that prohibited the formation of the more energically stable isomer. Similarly, the interconversion between isomers is frequently prohibited by the presence of a high potential barrier which cannot be crossed at room temperatures. In fact, the phenomena of irreversible thermochromism is just the case of two different stereoisomers in which the potential barrier is sufficiently low that the higher energy isomer can convert to the more stable isomer when $T > T_c$. Thus, thermochromic materials satisfy two criteria: different coordination geometries or isomers with comparable energies and the existence of a low potential barrier between the two geometries.

Chemical equilibrium, of course, depends upon two factors, energy and entropy. While energy criteria must be satisfied before thermochromic transitions are possible, it is clearly the entropy term which represents the driving force of the process. While the entropy may arise from a dissociation process, as in the dimer–monomer transitions, it more commonly arises from the onset of dynamic disorder of the organic component of the system. Thus, these transitions provide an opportunity to examine dynamic aspects of crystalline systems.

REFERENCES

1 B. Morosin and E.J. Graber, Acta Crystallogr., 23 (1967) 766.
2 N.S. Gill and R.S. Nyholm, J. Chem. Soc., (1959) 3997.
3 R.E. Caputo, S. Roberts, R.D. Willett and B.C. Gerstein, Inorg. Chem., 15 (1976) 820.
4 D.L. Coffen and T.E. McEntee, J. Org. Chem., 35 (1970) 503.
5 H.S. Preston, C.H.L. Kennard and R.A. Plowman, J. Inorg. Nucl. Chem., 30 (1968) 1463.
6 J. Reedijk and J. Verbiest, Transition Met. Chem., 3 (1978) 51.
7 G.J. Long and J.R. Ferraro, J. Chem. Soc., Chem. Commun., (1973) 719.
8 G.J. Long and D.L. Coffen, Inorg. Chem., 13 (1974) 270.
9 G.J. Long and E.O. Schlemper, Inorg. Chem., 13 (1974) 279.
10 G.J. Long and E.O. Schlemper, J. Chem. Soc., Dalton Trans., (1975) 96.
11 G.J. Long, G.L. Bertrand, D. Noel, S.H. Wu, K.G. Mayhan and D.L. Coffen, J. Chem. Soc., Dalton Trans., (1975) 762.
12 E.J. Laskowski, T.R. Felthouse, D.N. Hendrickson and G.J. Long, Inorg. Chem., 15 (1976) 2908.
13 S. Trofimenko, J. Am. Chem. Soc., 92 (1970) 51118.
14 H.S. Preston and C.H.L. Kennard, J. Chem. Soc. A, (1969) 2682.
15 H.S. Preston and C.H.L. Kennard, J. Chem. Soc. A, (1969) 1956.
16 H.S. Preston and C.H.L. Kennard, Chem. Commun., (1967) 708.
17 W.E. Hatfield, T.S. Piper and U. Klabunde, Inorg. Chem., 2 (1963) 629.
18 A.B.P. Lever, E. Mantovani and J.C. Donini, Inorg. Chem., 10 (1971) 2424.
19 L. Fabbrizzi, M. Micheloni and P. Paoletti, Inorg. Chem., 13 (1974) 3019.
20 P. Pfeiffer and H. Glaser, J. Prakt. Chem., 151 (1938) 134.
21 M.M. Andino, J.D. Curet and M.M. Muir, Acta Crystallogr., Sect. B, 32 (1976) 3185.
22 I. Grenthe, P. Paoletti, M. Sandstrom and S. Glikberg, Inorg. Chem., 18 (1979) 2687.
23 J.F. Ferraro, L.J. Basile, L.R. Garcia-Ineguez, P. Paoletti and L. Fabbrizzi, Inorg. Chem., 15 (1976) 2342.
24 H. Yokoi, M. Sai and T. Isobe, Bul. Chem. Soc. Jpn., 42 (1969) 2232.
25 A.B.P. Lever and E. Mantovani, Inorg. Chem., 10 (1971) 817.
26 M.B.G. Drew, D.M.L. Goodgame, M.A. Hitchman and D. Rogers, Proc. Chem. Soc., (1964) 363.
27 A. Bencini and D. Gatteschi, Inorg. Chim. Acta, 31 (1978) 11.
28 R.D. Willett, J.A. Haugen, J. Lebsack and J. Morrey, Inorg. Chem., 13 (1974) 2510.
29 G. Marcotrigiano, L. Menabue and G.C. Pellacani, Inorg. Chem., 15 (1976) 2333.
30 R.L. Harlow, W.J. Wells, III, G.W. Watt and S.H. Simonsen, Inorg. Chem., 13 (1974) 2106.
31 J.R. Ferraro and A.T. Sherren, Inorg. Chem., 17 (1978) 2498.
32 R.L. Harlow, W.J. Wells, III, G.W. Watt and S.H. Simonsen, Inorg. Chem., 14 (1975) 1768.
33 W.E. Hatfield and T.S. Piper, Inorg. Chem., 3 (1964) 841.
34 R.D. Willett, O.L. Liles, Jr., and C. Michelsoh, Inorg. Chem., 6 (1967) 1885.

35 D.W. Smith, Coord. Chem. Rev., 21 (1976) 93.

36 H. Remy and G. Laves, Ber. Bunsenges. Phys. Chem., 66 (1933) 401.

37 D.N. Anderson and R.D. Willett, Inorg. Chim. Acta, 8 (1974) 167.

38 P. Steadman and R.D. Willett, Inorg. Chim. Acta, 4 (1970) 367.

39 R.D. Willett, J.R. Ferraro and M. Choca, Inorg. Chem., 13 (1974) 2919.

40 D.R. Bloomquist and R.D. Willett, J. Am. Chem. Soc., 103 (1981) 2615.

41 M. Ahmed, M.S. Thesis, University of Cairo, 1975.

42 D.D. Swank, C.P. Landee and R.D. Willett, J. Magn. Magn. Mat., 15–18 (1980) 319.

43 (a) S.A. Roberts, Ph.D. Thesis, Washington State University, 1978.
(b) D.R. Bloomquist, Ph.D. Thesis, Washington State University, 1980.
(c) S.A. Roberts, D.R. Bloomquist, R.D. Willett and H.W. Dodgen, J. Am. Chem. Soc., 103 (1981) 2603.

44 R.D. Willett, J. Chem. Phys., 44 (1966) 39.

45 R.M. Clay, P. Murray-Rust and J. Murray-Rust, J. Chem. Soc., Dalton Trans., (1973) 595.

46 J.W. Woenk and A.L. Spek, Cryst. Struct. Commun., 5 (1976) 805.

47 D.D. Swank, C.P. Landee and R.D. Willett, Phys. Rev. B., 20 (1979) 2154.

48 D.R. Bloomquist, R.D. Willett and H.W. Dodgen, J. Am. Chem. Soc., 103 (1981) 2610.

49 S.H. Simonsen, personal communication.

50 S.A. Roberts, C.P. Landee and R.D. Willett, J. Chem. Phys., 68 (1978) 4574.

51 D.R. Bloomquist and R.D. Willett, Acta Crystallogr., Sect. B, 37 (1981) 1353.

52 V.L. Goedken, L.M. Vallarino and J.V. Quagliano, Inorg. Chem., 10 (1971) 2682.

53 C.E. Taylor and A.E. Underhill, J. Chem. Soc., (1969) 368.

54 P.J. Beadle, M. Holdstein, D.M.L. Goodgame and R. Grzeskowiak, Inorg. Chem., 8 (1969) 1490.

55 J.R. Ferraro and K.C. Davis, Inorg. Chim. Acta, 3 (1969) 685.

56 A. Sabatini and L. Sacconi, J. Am. Chem. Soc., 86 (1964) 17.

57 A.T. Sherren and J.R. Ferraro, Inorg. Chim. Acta, 22 (1977) 43.

58 C.P. Landee and R.D. Willett, unpublished results.

59 M.N. Hughes and K.J. Rutt, Inorg. Chem., 10(2) (1971) 414.

60 S. Mitra, T. Yoshikuni, A. Uehara and R. Tsuchiya, Bull. Chem. Soc. Jpn., 52(9) (1979) 2569.

61 B.P. Sudha, N.S. Dixit and C.C. Patel, Indian J. Chem., Sect. A, 16 (1978) 771.

62 H. Bassett and R.G. Durrant, J. Chem. Soc., (1922) 2630.

63 A.A.G. Tomlinson and B.J. Hathaway, J. Chem. Soc. A, (1968) 2578.

64 Y. Mori, H. Inoue and M. Mori, Inorg. Chem., 14 (1975) 5.

65 G.G. Aleksandrov, Y.T. Struchkov, A.A. Kurganov, S.V. Rogozhin and V.A. Davankov, Inorg. Nucl. Chem. Lett., 10 (1974) 959.

66 L.B. Battaglia, A.B. Corradi, G. Marcotrigiano, L. Menabue and G.C. Pellacani, J. Chem. Soc., Dalton Trans., (1981) 8.

67 G.C. Pellacani, personal communication.

68 E.A. Heintz, Inorg. Nucl. Chem., 21 (1961) 64.

69 H. Hahn, G. Frank and W. Klingler, Z. Anorg. Allg. Chem., 279 (1955) 271.

70 C.E. Olsen and P.M. Harris, Phys. Rev., 86 (1952) 651.

71 R.W. Asmussen and P. Anderson, Acta Chem. Scand., 12 (1958) 939.

72 P.K. Kadaba and D.E. O'Reilly, J. Chem. Phys., 55 (1971) 5833.

73 E. Caventou and E. Willm, Bull. Soc. Chim. Fr., (11)13 (1870) 194.

74 J.S. Chivian, R.N. Clayton, D.D. Eden and R.B. Hemphill, Appl. Opt., 11 (1972) 2649.

75 J.S. Chivian, Mater. Res. Bull., 8 (1973) 795.